Scattering of cold electrons by ammonia, hydrogen sulfide, and carbonyl sulfide

N. C. Jones,[1] D. Field,[2,*] S. L. Lunt,[3] and J.-P. Ziesel[4]
[1]*Institute for Storage Ring Facilities (ISA), University of Aarhus, DK-8000 Aarhus C, Denmark*
[2]*Department of Physics and Astronomy, University of Aarhus, DK-8000 Aarhus C, Denmark*
[3]*Kittiwake Developments Ltd, Littlehampton, West Sussex BN17 7LU, United Kingdom*
[4]*Laboratoire Collisions Agrégats Réactivité (CNRS-UPS UMR5589), Université Paul Sabatier, 31062 Toulouse, France*
(Received 2 July 2008; published 29 October 2008)

Experimental data obtained with a high-resolution transmission experiment are presented for the scattering of electrons in the energy range 20 meV–10 eV for NH_3, 25 meV–10 eV for H_2S, and 15 meV–2.5 eV for OCS. Data include cross sections for both integral scattering and scattering into the backward hemisphere, the latter up to 650 meV impact energy, with an electron energy resolution of between 1.6 and 3.5 meV. The new data allow the first detailed comparison with theory for the energy regime dominated by rotationally inelastic and elastic scattering for these species. It is evident that theory still lacks quantitative predictive power at low energy, although qualitative agreement is consistently good for all three species. A discussion is given of the possible presence of a virtual state in OCS scattering as recently proposed on theoretical grounds.

DOI: 10.1103/PhysRevA.78.042714 PACS number(s): 34.80.−i

I. INTRODUCTION

The work presented here deals primarily with the very low-energy regime for collisions of electrons with NH_3, H_2S, and OCS. Collisions are essentially in the cold regime in which the wavelength of the incident electrons is very much greater than the range at which there is significant interaction between the electron and the molecule. There exist no data in the literature for these species for scattering below 400 meV, whereas the present data extend down to 15–25 meV. At the lowest energies, scattering is strongly dominated by elastic and rotationally inelastic events, with the long-range dipole interaction generating very large cross sections. Thus, as originally predicted by theory [1–3], cross sections for rotationally inelastic scattering can achieve values of many hundreds of $Å^2$ for electron impact energies of a few tens of meV. This was first verified experimentally in [4] and subsequently in [5–12] for a variety of polar species.

There remain rather few data in the literature that deal with rotational excitation of polar molecules near threshold [13]. This paucity of data reflects the practical difficulties attendant on the measurements. The subject of rotational excitation of polar molecules by low-energy electrons is, however, one of considerable practical and theoretical interest. Radio-Frequency (rf) discharges used in microelectronic device manufacture frequently employ process gases that are polar species, for example halogenated hydrocarbons. Rotationally inelastic scattering of electrons with these species and their reactive fragments are a major factor in determining the electron temperature in rf plasmas. This in turn influences the abundance of negative ions in these plasmas and thereby the electrical characteristics of rf systems, affecting the energy with which ions strike the substrate, a defining quantity in plasma manufacturing techniques [14,15]. Inelastic scattering by polar molecules is also important in planetary atmospheres and in astrophysical plasmas. For example, in the astrophysical context, cooling of electrons by polar species such as H_2O makes a major contribution in reducing the electron temperature to the ambient value of 10–20 K [16]. This enhances the rate of recombination of electrons with molecular cations, the final stage in the gas phase production of the great majority of interstellar species, and also has an influence on the manner in which electrons may penetrate the water ice mantle of interstellar grains [17].

With regard to the theory of rotational scattering, very considerable advances have been made in the *ab initio* field, with respect, for example, to scattering by H_2O [18,19] and for all three species represented here [20–27] as discussed in detail below. A general theoretical basis, used presently only for H_2O, has recently been developed through which rotational state-to-state cross sections and elastic cross sections can be extracted from laboratory data for electron transmission [11]. We refer to concepts invoked in [11] in our discussion of scattering by OCS below.

The present work proceeds first by introduction of the experimental method. Data for NH_3, H_2S, and OCS are then presented over the energy range between close to zero energy up to 10 eV for NH_3 and H_2S and to 2.5 eV for OCS. A comparison with existing data in the literature is given for each species, revealing a number of serious discrepancies at energies below a few eV. Comparison with theory, including the first-order-Born point dipole approximation, is also given. This includes a more extended discussion of low-energy scattering in OCS.

II. EXPERIMENTAL METHOD

The experimental system has been described in detail in [28–30]. Electrons are formed by photoionization of Ar using focused monochromatized synchrotron radiation at the sharp autoionizing resonance Ar^{**} $3p^5$ $(^2P_{1/2})11s$ superposed on the broad $9d'$ resonance at 78.65 nm [31], ~4 meV above the $^2P_{3/2}$ ionization threshold. Both the ASTRID storage ring at the University of Aarhus and the

*Author to whom correspondence should be addressed. dfield@phys.au.dk.

SRS at Daresbury Laboratory were used to obtain data. The energy resolution of the photoelectrons is determined by the resolution in the photon beam via the performance of the beamline monochromator [28,30]. The resolution used in the present work was 3.5 meV full width at half maximum (FWHM) for NH_3 and H_2S (Daresbury) and 1.6 meV FWHM for OCS (ASTRID). Electrons are formed into a beam and pass through room-temperature samples of the target gases contained in a collision cell of length 30 mm, entrance hole diameter 2 mm, and exit hole 3 mm. The intensity of the electron beam, in the presence and absence of target gas, is recorded at a channeltron as a function of electron energy. The cross section for electron-molecule encounters is derived via $\sigma_{T,I}=(Nl)^{-1}\ln(I_0/I_t)$, where N is the target gas number density, l is the path length in the gas, and I_0 and I_t are, respectively, the intensities of the incident and transmitted electron beams. This yields the variation of the total integral scattering cross section, $\sigma_{T,I}$, where "total" refers to all events—elastic, inelastic, and reactive—and "integral" to integration in principle over the full 4π sr. The problem of the nondetection of small-angle forward scattered electrons is discussed in Sec. II A. The pressure in the target cell was measured using a capacitive manometer (Edwards 655) for NH_3 and H_2S and with a Leybold rotating ball gauge (Viscovac VM212) for OCS.

In independent measurements, an axial magnetic field of strength $\sim 2\times 10^{-3}$ T is introduced. In the presence of the axial magnetic field, any electrons scattered into the forward hemisphere by the target gas are realigned to perform forward-moving helical trajectories around the axis of the field and are detected as unscattered. All electrons scattered in the backward hemisphere follow backward-moving trajectories around the direction of the magnetic field. These electrons are lost to the incident beam. The apparatus then determines cross sections for scattering between 90° and 180°, that is, total backward scattering cross sections, σ_b. Above a certain energy, in the presence of the magnetic field, electrons scattered at close to 90° have sufficient transverse energy to cause them to move in a spiral path with a diameter such that they cannot pass through the exit hole of the target gas cell. For electrons on axis, this energy is ~800 meV, but the energy is lower for off-axis incident electrons. In order to determine the energy to which absolute backward scattering cross sections are reliable, the backward cross section was measured in N_2 and compared with differential cross sections given in [32] integrated between 90° and 180°. Good agreement is found up to ~700 meV. The experimental technique for the determination of σ_b has been very thoroughly checked in previous work, e.g., [7,8,30,33].

As a check on the accuracy of the cross sections, in addition to the above data, long integration time experiments were carried out at between 5 and 10 fixed energies spanning the range of interest. In these experiments, electron counts were typically accumulated for 2 min both with and without the gas present, with continuous monitoring of the pressure and the intensity of the synchrotron radiation. This process was repeated five or more times at each energy. There was generally very good agreement between the cross sections obtained in this manner and those obtained through scanning the electron energy.

The absolute electron energy scale is calibrated by observing the peak in the $N_2^-\ ^2\Pi_g$ resonance around 2.44 eV. Results in [34–36] indicate that the peak recorded in the total cross section at ~2.44 eV is a good energy calibrator for both total and backward-scattering data, and thus for experiments with and without the magnetic field present. We assign an energy of 2.442 eV to this peak, this figure being the average of the values of 2.444 and 2.440 eV in [34,35], respectively. Discrepancies between the N_2 resonance energy and electron energies estimated from potentials in the system lay typically between 10 and 70 meV, and did not vary significantly over the course of many experiments. In the energy regime of a few tens of meV, reported values of electron energies are accurate to between ±1 and ±2 meV [10,30].

Random errors in the reported cross sections arise from sources including pressure measurements, random fluctuations in the electron beam intensities and uncertainties in calibration of the path length of the electrons through the collision cell. These uncertainties correspond to an error of ±5% (one standard deviation) in the quoted cross sections at all energies for scattering in the presence or absence of the magnetic field, save at the very lowest energies in the absence of the magnetic field, that is, for total integral cross sections, for which a figure of ±8% is appropriate. Systematic errors arising from the omission of a proportion of the forward scattering cross section are discussed below.

A. Contributions to measured cross sections at low energy

The geometry of the collision chamber dictates that in our measurements of nominally integral cross sections, we omit to record a part of the cross section associated with low-angle scattering. The geometry of the experiment is precisely defined. Thus omission of low-angle forward scattering has no impact on comparison with theory, since theory may exclude any specified angular range, as implemented in [11] and as we describe below. The effect of omission of forward scattering is most marked at higher energy. Thus at 30 meV impact energy for OCS and NH_3, 36% and 11.5% of the rotationally inelastic scattering is omitted in our measurements, respectively. At 100 meV, the omission is 51% for OCS and 25% for NH_3, where all figures were obtained using Born angular distributions.

The problem of the nondetection of forward scattering has been dealt with at some length in [6,37]. We follow the method used in these references in order to calculate the effective rotationally inelastic Born cross sections. The theory of rotational excitation by slow electrons using the first Born pure dipole approximation has been reviewed in [2,3]. For the case of ammonia, we use an expression developed in [1] and re-expressed in [6]. In order to proceed, we make the assumption that any stray fields in the interaction zone are negligible and therefore that the ability to detect forward scattered electrons is governed purely by the geometry of the cell. We refer to the polar half-angle omitted for scattering into the forward direction at any point along the collision chamber as θ_1. In order to compare the predictions of the Born theory with experimental results, theoretical values are estimated using a range of values of θ_1, appropriate

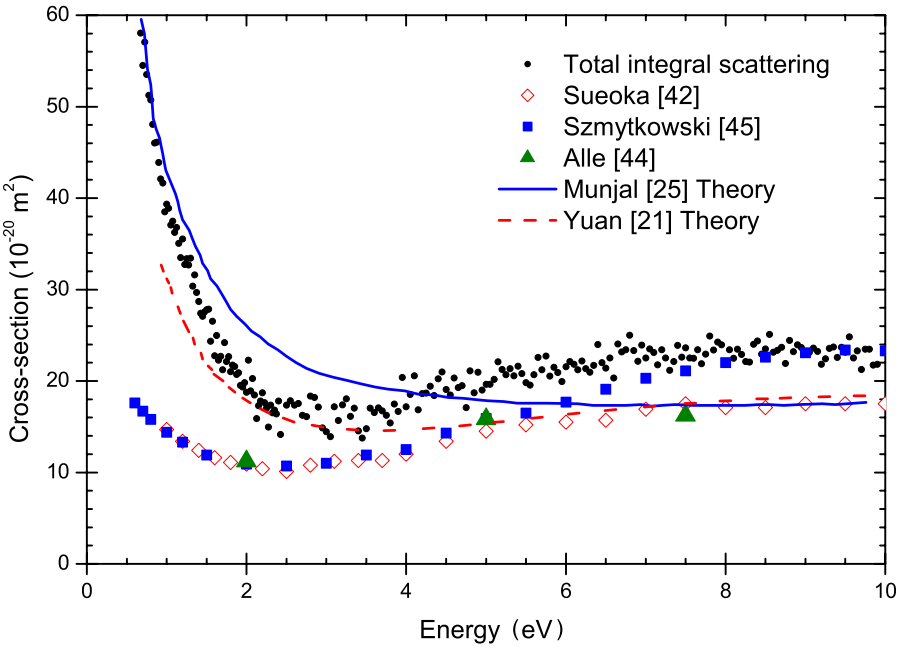

FIG. 1. (Color online) NH_3: the variation of the sum of the integral elastic and inelastic cross sections, $\sigma_{T,I}$, between 0.675 and 10 eV. Also shown are experimental data from Sueoka *et al.* [42], Szmytkowski *et al.* [45], and Alle *et al.* [44] and theoretical values from Munjal *et al.* [25] and Yuan *et al.* [21].

to the length of the cell and the apertures in it. We use a coarse numerical integration, for each chosen point within the collision chamber using an appropriate value of the angle θ_1 with the other angular limit set to π. This corrected cross section may be expressed as $l^{-1}\int_0^l dl[\sigma_{\mathrm{Born}}]_{\theta_1}^{\pi}$, where σ_{Born} is the cross section calculated from Born theory for incoming on-axis electrons for the appropriate value of l (which dictates the value of θ_1). σ_{Born} includes a factor of 2π for integration over the azimuthal angle about which the scattering is symmetric. We have used nine values of θ_1 between 3° and 27°, corresponding to a set of equidistant points along the collision chamber. All calculations of the Born scattering cross section reported here involve this effective reduction in the full angular range. Note that in our experiment, we record both elastic and rotationally inelastic scattering and we are not able to distinguish between the two.

Other processes that may occur at low energy are threshold vibrationally inelastic scattering and quadrupole scattering. No threshold vibrational excitation is discernible in any of the three species studied. There appear to be no studies in the literature of threshold vibrational excitation of NH_3. Vibrationally inelastic scattering has, however, been recorded in H_2S near threshold [38] at 0.4 eV. Integral cross sections for the sum of the symmetric and antisymmetric stretch are of the order of 2 Å^2. OCS vibrational excitation, at respective threshold values of 64, 107, and 256 meV for the bend, symmetric, and antisymmetric stretch, has been recorded in crossed-beam experiments (unpublished data) but are evidently of too low cross section to be detected in the transmission spectra within our signal to noise. The quadrupole contribution to the scattering cross sections [39] may be estimated to be no greater than 1 Å^2 for the case of the species with the largest quadrupole moment, namely H_2S (Q= −4.71 a.u. [40]). In addition, none of the three species shows any evidence of long-lived attachment or dissociative attachment at low energy.

III. RESULTS AND DISCUSSION

In this section, we report our results and compare these data with experimental and theoretical values obtained by other groups. A general point is that the polar species measured here are known to show strong forward scattering throughout the relevant energy range and not only at very low energy where rotationally inelastic scattering dominates. This has been illustrated experimentally for NH_3 for example in [44], for H_2S in [47], and for OCS in [54]. The different experimental geometries used by different groups therefore contribute to the discrepancies between values reported in the literature and to discrepancies between theory and experiment. Quantitative comparison, therefore, becomes difficult for integral cross sections, and it is doubtful if such comparisons are valid; however, for the record we report how close, in approximate percentage terms, the present values lie to those reported earlier. In this connection, we emphasize how important it is that theoretical groups, in comparing their results for example with our data at very low energy, take account of the omission of a solid angle using the method outlined in Sec. II A.

A. NH_3

Experimental data for scattering cross sections for NH_3 (purity >99.9%) are shown in Figs. 1 and 2, the former showing data between 0.4 and 10 eV and the latter the low-energy region up to 500 meV.

Earlier experimental work on NH_3 in the few eV range shows significant discrepancies for values of the integral scattering cross section between different laboratories of factors of 1.5–2 at energies between 4 and 10 eV. This is illustrated in [41] citing data from [42–45]. The form of the variation of the cross section between 1 and 10 eV is, however, generally well determined, with a weak minimum around 2.5 eV. Cross sections reported in [42,43,45] agree

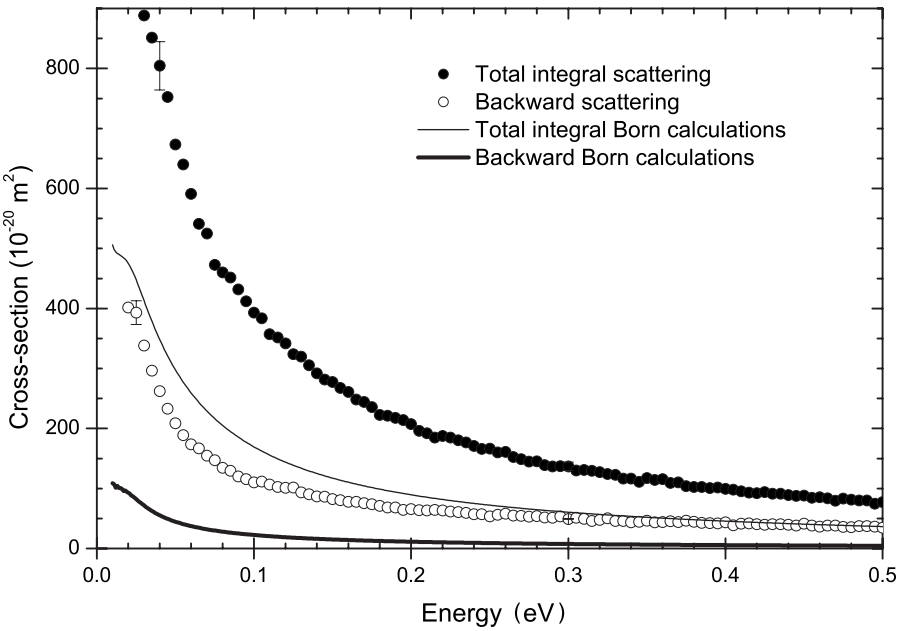

FIG. 2. NH_3: upper set: the sum of the integral elastic and inelastic cross sections measured in the absence of an axial magnetic field, between 15 and 500 meV. Lower set: the elastic and inelastic backward scattering cross section into the backward 2π sr, obtained in the presence of the axial magnetic field, between 14 and 500 meV. Also shown are Born integral cross sections, allowing for omission of forward scattering (see Sec. II A) and the first-order point dipole Born values for scattering into the backward 2π sr.

with those reported here within 10–20% or better at energies >7 eV. Disagreement is >30% with values in [44] at 7.5 eV, where integral cross sections were constructed by extrapolation of differential data. The authors note the uncertainties attendant upon such extrapolation. Discrepancies between the present results and those in [45] are especially severe at the lowest energies of 0.8 eV for which those authors report data. A value of 51 Å^2 is reported in the present work at this energy, whereas [45] reports 18 Å^2.

Data reported here, showing high values of cross section at low energy, give support to the theoretical estimates of integral cross sections in [20–22,25], which use a broad range of theoretical methods. The results in [21] are especially clear in this respect since estimates are given of cross sections omitting scattering within the forward zero to 5°. This roughly mimics our experiment. Thus at 1 and 2 eV, cross sections are given in [21] of 33 and 18 Å^2, where we measure 40 and 19 Å^2. The most recent estimates in [25] are 43 and 26 Å^2, respectively, at these energies but without omission of forward scattering.

No theory probes energies below ~0.7 eV. In Fig. 2, we compare our data with values derived from the first-order point dipole Born approximation using the standard expression for the symmetric top, e.g., [1,3,46]. Theoretical estimates based upon Born are of the rotationally inelastic part of the cross section only and omit the elastic scattering. Born estimates should therefore lie below measured values, as seen in Fig. 2. The difference between Born and the observed value may give an approximate estimate of the elastic-scattering contribution. On this basis, the proportion of elastic scattering appears to remain roughly constant at ~55% between 500 and 30 meV. For comparison, the proportion of elastic scattering in H_2O at 200 meV is ~25% [11,18]. Backward scattering appears strongly underestimated by Born. At face value, Born cross sections suggest 88% elastic at 500 meV falling slowly to 79% at 25 meV. These results for both integral and backward scattering, and comparison with Born, point to an important contribution from the repulsive short-range part of the electron-NH_3 interaction potential. This is especially clear from the backward data since the repulsive wall of the interaction potential plays a larger role in scattering into backward angles.

B. H_2S

Experimental results for cross sections for H_2S (Aldrich, >99.5%) are shown in Figs. 3 and 4, the former showing data between 380 meV and 10 eV and the latter the low-energy region up to 650 meV.

There have been three experimental reports of the integral scattering cross section for H_2S at low energy [47–49], where [47] provides estimates from differential values. These data are shown in Fig. 3. Agreement with the present data and the cross sections in [48,49] between 1.5 and 5 eV is acceptable. Above 5 eV, Refs. [48,49] find increasingly larger values of cross section than in the present work or in [47], culminating in a discrepancy of 25% at around 9.5 eV. There are no lower-energy experimental data available for comparison.

The most recent theoretical results are those of [26] in which earlier work is reviewed. The older results of [50] appear in good accord with our data. The B_2 resonance is found at around 2 eV, as observed experimentally, and elastic and rotationally inelastic scattering is approximately reproduced down to the lowest energies for which cross sections are calculated of ~0.46 eV. The results of [26] show the correct qualitative behavior but obtain the B_2 resonance at around 3.9 eV. Moreover, calculated values between 0.5 and 0.25 eV, the lowest energies reported, are considerably in error. This may clearly be seen in Fig. 4, where both the tail-end of results in [50] and the low-energy data in [26] are included for comparison. Discrepancies at very low energy are greater than shown since the calculated values include all forward scattering whereas the experimental data do not. Theoretical estimates reported in [51], omitted for clarity in Fig. 3, are generally close to those reported in [26,50], with

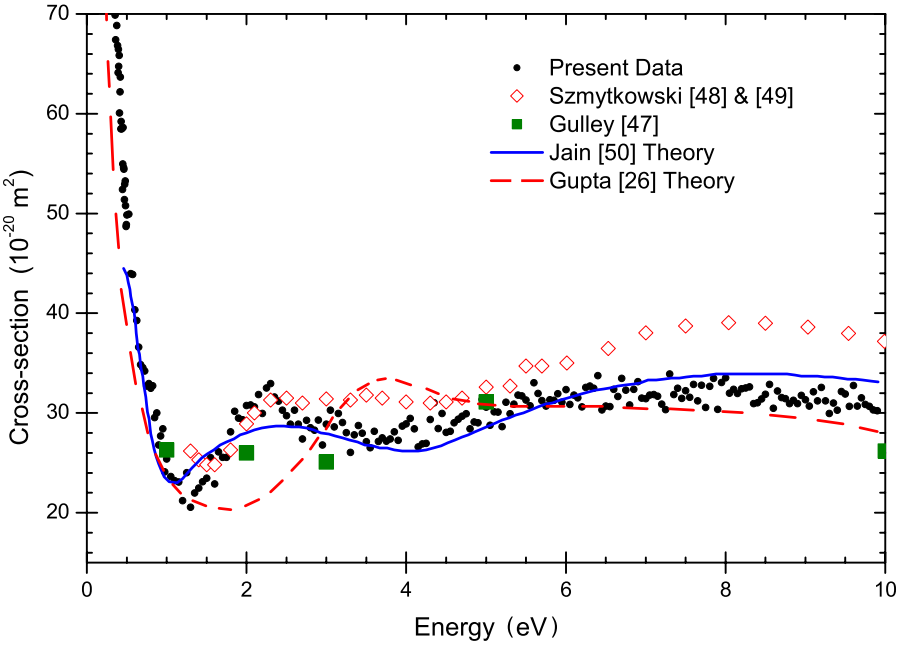

FIG. 3. (Color online) H_2S: the variation of the sum of the integral elastic and inelastic cross sections, $\sigma_{T,I}$, between 380 meV and 10 eV. Also shown are experimental data in Szmytowski *et al.* [48,49] and Gulley *et al.* [47] and theoretical values from Jain *et al.* [50] and Gupta *et al.* [26].

the B_2 resonance at ~3 eV, lying between the values reported in [26,50].

C. OCS

Experimental results for cross sections for OCS (Aldrich, >97.5%) are shown in Figs. 5 and 6, the former showing data from 39 meV to 2.5 eV and the latter the low-energy region up to 500 meV in more detail and to lower energy.

Earlier experimental data in the low-energy regime for total scattering may be found in [52–56]. With reference to Fig. 5, the data of [53] agree within ~25% or better with the present data down to energies of 0.4 eV. The values reported in [55] probably suffer from a lack of resolution at low energy, hence blurring out the 1 eV shape resonance. Data in [54] were obtained from summing differential cross sections with extrapolation to include all angles. There is agreement within 25% at the peak of the shape resonance at ~1.2 eV and at 2.5 eV. At 0.6 eV, a large discrepancy arises, at least in part because [54] effectively includes the forward scattering omitted in our data. An estimate from Born suggests that in our data at 0.6 eV we may be omitting to detect ~60% of the scattering cross section.

Recent theory may be found in [23,24,27]. Values from these calculations may be found in Figs. 5 and 6. Evidently the magnitude, width and position of the Π shape resonance are somewhat in error. Agreement at low energy, seen in Fig. 6, is again more qualitative than quantitative, given that the calculations involve all 4π sr and the experiments omit a significant fraction.

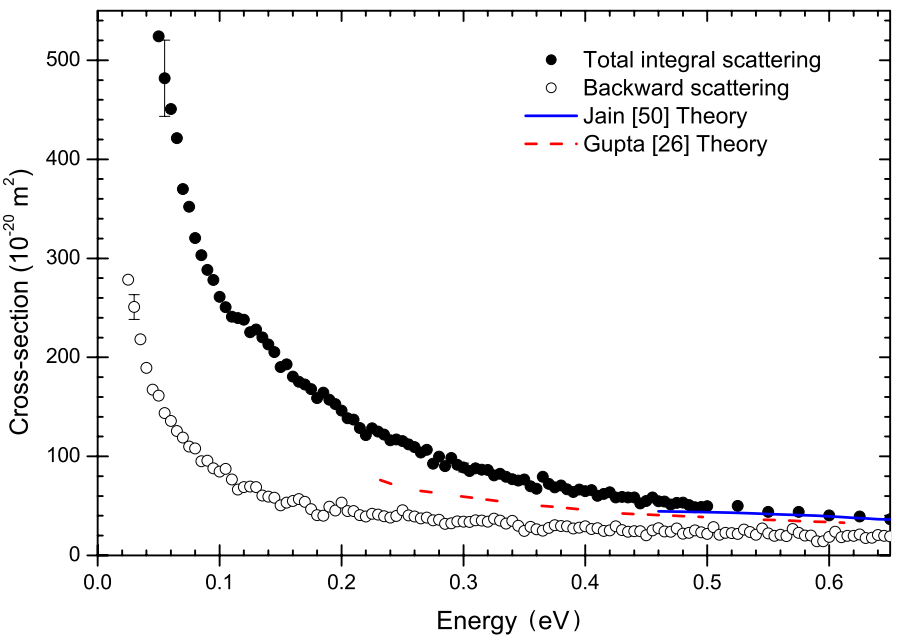

FIG. 4. (Color online) H_2S: upper set: the sum of the integral elastic and inelastic cross sections measured in the absence of an axial magnetic field, between 15 and 500 meV. Lower set: the elastic and inelastic backward scattering cross section, into the backward 2π sr, obtained in the presence of the axial magnetic field, between 14 and 500 meV. Also shown are the lower energy theoretical values of integral cross sections from Jain *et al.* [50] and Gupta *et al.* [26].

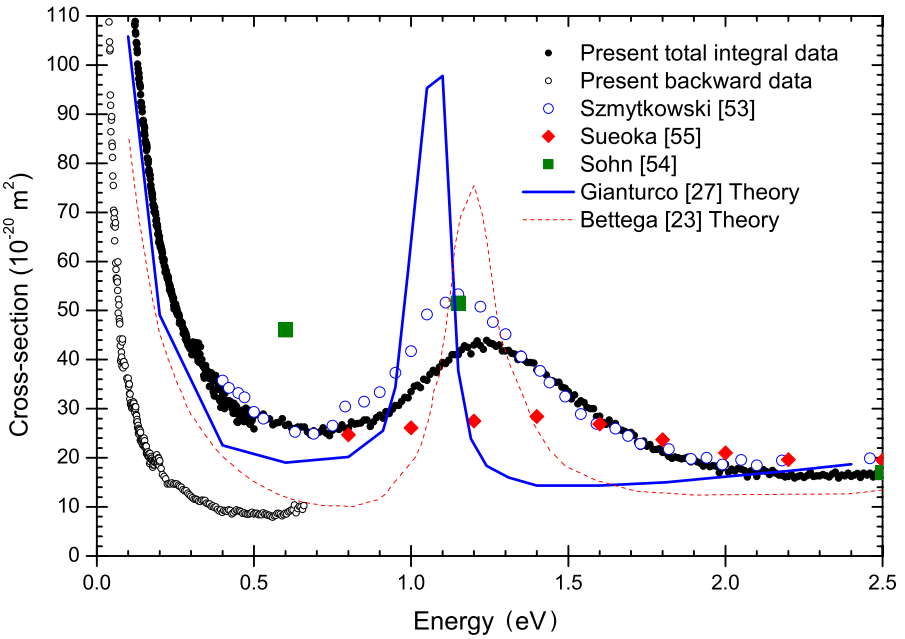

FIG. 5. (Color online) OCS: the variation of the sum of the integral elastic and inelastic cross sections, $\sigma_{T,I}$, between 120 meV and 2.5 eV, and the elastic and inelastic backward scattering cross section into the backward 2π sr, between 39 and 650 meV. Also shown are experimental values from Szymtkowski *et al.* [53], Sueoka *et al.* [55], and Sohn *et al.* [54] and theoretical values of integral cross sections from Gianturco *et al.* [27] and Bettega *et al.* [23].

In [23,24,27], the interesting proposal has been made that a Ramsauer-Townsend minimum and a virtual state may be present in low-energy scattering by OCS. These two features go hand-in-hand. The presence of a Ramsauer-Townsend minimum implies a negative *s*-wave scattering length, which is a prerequisite for the involvement of a virtual state at zero energy. One diagnostic of a virtual state derives from the angular distribution of scattered electrons at very low energy, which should become increasingly isotropic as the energy falls [29]. Our data for integral scattering extend to 22 meV for OCS. At this energy, the ratio of the backward to the integral cross section is 0.56. Since some proportion of the forward scattering is omitted, the true figure is lower. Using the Born angular distribution and assuming that this is similar for both rotationally inelastic and elastic scattering, the true ratio of backward to integral scattering evidently exceeds 0.4. Our data are therefore consistent with backward-forward symmetry at energies approaching zero. Coupled with a high cross section, this is reminiscent of a virtual state and cannot be readily reconciled with dipole scattering.

A discussion of possible virtual state scattering and the Ramsauer-Townsend effect in OCS

Virtual state scattering in molecular collisions was first described experimentally in [29] for CO_2 and subsequently for benzene [57], C_6F_6 [58], and CS_2 [59]. Note that in each case these molecules possess zero dipole moment. We return to this aspect below but consider first whether a virtual state, in the conventional sense of a pure *s*-wave event, is possible in OCS in terms of the lowest unoccupied molecular orbital (LUMO) symmetry. The requirement is that the character of

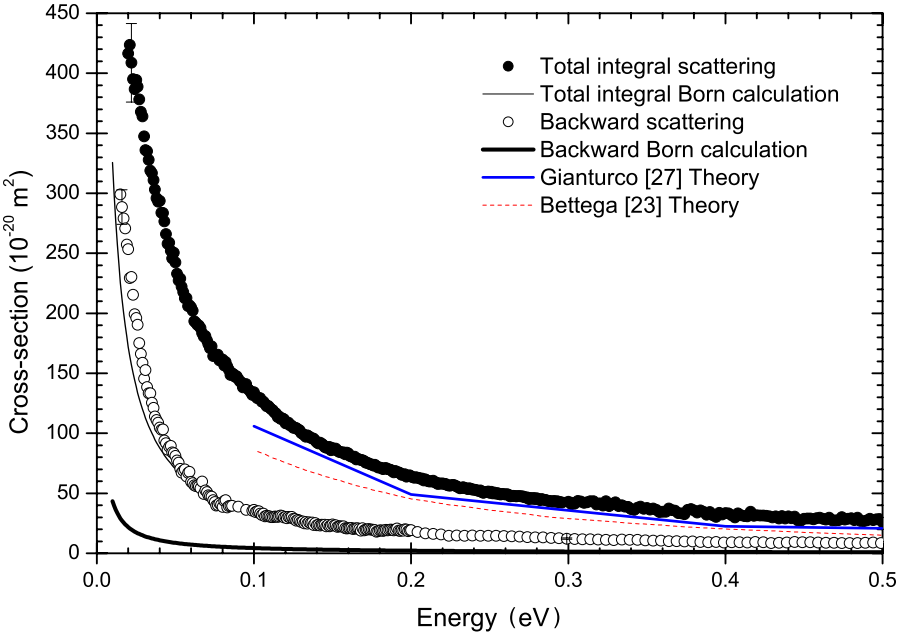

FIG. 6. (Color online) OCS: upper set: the sum of the integral elastic and inelastic cross sections measured in the absence of an axial magnetic field, between 15 and 500 meV. Lower set: the elastic and inelastic backward scattering cross section into the backward 2π sr, obtained in the presence of the axial magnetic field, between 14 and 500 meV. Also shown are the lower-energy theoretical values of integral cross sections from Gianturco *et al.* [27] and Bettega *et al.* [23] and values obtained using the first-order point dipole Born approximation.

the state of the LUMO must be totally symmetric to all operations of the relevant point group.

Excited states of OCS in the linear configuration are $^1\Sigma^-$, $^1\Delta$, and $^1\Sigma^+$. Using neutral orbitals as a guide [60], the LUMO of OCS is the $^1\Sigma^-$ state, lying very close in energy to the $^1\Delta$ state. The $^1\Sigma^+$ state lies at considerably higher energy. As the electron approaches, OCS^- bends in order to stabilize the temporary negative ion, as do CO_2 and CS_2 [61,62]. In so doing, the Σ^- state achieves an A'' symmetry in the relaxed C_s symmetry of bent OCS^-. This state does not accept an s wave. The Σ^- state under $C_{\infty v}$ is also incompatible with an s wave. However, the Δ state achieves an A' symmetry that will accept an s-wave under C_s, though not when linear under $C_{\infty v}$. Thus there are low-lying orbitals available for virtual state formation since the molecule bends. Virtual state formation would therefore be via the indirect mechanism in which nuclear motion is necessary [58].

The theoretical results presented in [23,24,27] show the variation of the phase shift as a function of energy of that part of the wave that has the species Σ under $C_{\infty v}$. This shows the dominance of the Σ component of partial waves—s waves according to [24]—at low energy. The phase shift is found to pass through zero at around 1 eV in [24] and ~0.6 eV in [27]. This behavior is reminiscent of that encountered in nonpolar target species with a negative scattering length and may give rise to a Ramsauer-Townsend effect. Now, despite many years of promises and great improvements in the treatment of nonlocal electronic effects, these theories still work in a fixed nuclei approximation. The results in [23,24,27] are therefore potentially misleading. Σ symmetry exists only under $C_{\infty v}$. Results in [61,62] show, as mentioned above, that the nuclear framework of OCS will bend as the electron approaches, the negative ion becoming adiabatically stable upon bending to ~152° if it has the time to sample such configurations. Therefore, theory should identify components of A' symmetry, which transform as s waves under the relaxed C_s symmetry of the bent anion, not those of Σ symmetry.

We turn now to the problem that OCS has a significant dipole moment (0.712 D). Both [24,27] refer to the increase of the s-wave phase shift as the electron impact energy drops. Since the long-range field is dipole, higher partial waves are not excluded at low energy. All partial waves are involved at all energies and all partial waves are mixed. This arises because the potential and the centrifugal potential share an r^{-2} dependence. This is indeed why [27] refers in their figure 2 to the Σ symmetry component of the scattered wave. In fact, [27] appears to be invoking a new definition of virtual state scattering and of the Ramsauer-Townsend effect involving Σ symmetry components rather than pure s waves [29,63], albeit within the incorrect symmetry as discussed above.

We propose a conceptually different approach from that presented in [23,24,27]. This is only outlined here and should be viewed as a tentative proposal for future and rigorous investigation. [11] showed how dipole harmonics can be used as a very effective basis for scattering in a long-range dipole field. Dipole harmonics are weighted linear combinations of spherical harmonics, where the weighting depends on the dipole moment of the target. Dipole harmonics are constructed as eigenfunctions of the Hermitian operator $L^2 - 2D\cos\theta$ where θ is the angle between the dipole moment vector and the position vector of the scattered electron. The resulting σ-, π-, δ-, … waves, therefore, form an orthonormal set that may thus be used as a basis for scattering on the core potential. Just as in the standard problem in which a short-range potential excludes higher partial waves at low energy, all waves other than σ dipole harmonics are increasingly turned away by a 'centrifugal-like' potential as the impact energy becomes lower. Thus at low energies, there is a dominance of σ waves. One may therefore invoke behavior in which the σ-wave phase shift passes through $n\pi$ at some low energy yielding a Ramsauer-Townsend-like minimum in the elastic and rotationally inelastic cross section. Thus the minima in the cross section at 720 meV in the integral and 540 meV in the backward scattering in Fig. 5 could be due to a zero in the σ-wave phase shift. If this is so, the scattering is not pure σ-wave—as one would indeed expect at these energies [11]—since there is considerable cross section even at the deepest point of the minimum. In this model, this arises from the involvement of π and δ waves and in principle higher waves. There naturally remains the possibility that the observed dips in the integral and backward scattering cross sections arise from a fall-off from the Π-type resonance at 1.24 eV and cannot be ascribed wholly—or even in part—to a Ramsauer-Townsend effect.

Turning to the issue of virtual state scattering in OCS, this again turns on the dipole field involved. Reference [64] showed that a virtual state may survive with a target dipole of <1.19 D. For this purpose, only the s wave was retained in the analysis on the basis that the near-spherical symmetry of the outgoing wave is preserved for low enough dipole moments. We would propose that one should be able to develop a more rigorous approach in which one retains only the σ dipole harmonic wave, yielding a more complete description of the nature of virtual state scattering in the presence of a dipole field (in the absence of dipole bound states [65]). This in turn suggests a modified version of effective range theory. In fact, such a theory has already been developed for dipolar species but using standard spherical harmonics [66]. Here we suggest a simple ansatz to effective range theory, in which the s-wave phase shift is replaced by a σ-wave phase shift and the s-wave scattering length by a σ-wave scattering length, A_σ. By extrapolation of the OCS data from the value of 299 $Å^2$ at the lowest measured energy of 15 meV to zero energy for the backward data, we estimate a zero-energy backward cross section of 500 ± 25 $Å^2$. This gives an integral value of 1000 ± 50 $Å^2$ and thus a value of A_σ of 17 ± 1 a.u. Note that as we move to very low energy, the adiabatic approximation, fundamental to [11], will break down and moreover only rotationally superelastic channels will remain open in the limit. By analogy with [58,67], the virtual state, that is, the OCS^- moiety in the continuum, lies at an energy of $(2A_\sigma)^{-1}$ above the neutral. On this basis, we would therefore suggest that the virtual state lies unbound by $\sim 50 \pm 5$ meV. This is in agreement with the qualitative statement in [62], which gives a value of the electron affinity in the fully relaxed configuration of 'either slightly negative or zero' and is also consistent with the value reported in [68] of −7 meV. Reference [61] gives a rather more negative

value of -220 meV. The value that we quote of -50 ± 5 meV should be seen as an average over all those trajectories and associated lifetimes, and thus bent states of OCS, which are sampled by the superposition of events that make up the scattering process. Our value would be expected to be somewhat more negative than the negative diabatic affinity associated with the fully relaxed state of OCS^- [62].

In addition, we note that OCS does not show the strong vibrational effects seen in CS_2 [59] because adiabatically bound states of OCS^- are not so readily achievable as the corresponding states in CS_2^-. Thus OCS has to bend through nearly 30° to bind the electron adiabatically [62], whereas CS_2 has to bend through only ~10° [61].

IV. CONCLUDING REMARKS

We summarize our conclusions as follows.

(i) Our data provide new and reliable values of cross sections for scattering of NH_3, H_2S, and OCS into the very low-energy regime in which rotational excitation becomes the strongly dominant inelastic process.

(ii) These data are valuable for comparison with *ab initio* theory and give a clear indication of the reliability of cross sections calculated in this energy regime, using, for example, the Schwinger variational method and *R*-matrix techniques [13]. Despite the success with H_2O [11,18], it is evident that theory has not generally achieved the predictive power in which quantitative credence can be given to rotationally inelastic scattering for species whose cross sections are not amenable to measurement. These include radicals and other highly reactive species typically encountered in rf discharges in planetary atmospheres or in the interstellar medium.

(iii) Data for these three species are susceptible to analysis using the theory set out in [11]. Thus it should be possible in the future to extract rotational state-to-state cross sections from the data presented here.

(iv) There is some experimental evidence for a virtual state in OCS scattering, as suggested in [23,24,27]. This, however, requires further theoretical investigation involving bent states of the system in C_s symmetry.

ACKNOWLEDGMENTS

The authors would like to thank Dr. R. J. Gulley for his help in obtaining some of the data reported here for NH_3 and H_2S. D.F. would like to acknowledge support by the Danish National Research Foundation through the research centre ACAP (Aarhus Centre for Atomic Physics) and support from the Danish Natural Science Research Council (SNF, now FNU). N.C.J. would like to thank the EU EPIC Network. J.P.Z. would like to thank the CNRS and SNF for support under the Science Exchange Programme and the EU under the Access to Research Infrastructure programme. We would also like to thank the Directors and Staff at both the Institute for Storage Ring Facilities at Aarhus (ISA) and at the SRS, Daresbury Laboratory for providing the facilities necessary for this work.

[1] O. H. Crawford, J. Chem. Phys. **47**, 1100 (1967).
[2] K. Takayanagi and Y. Itikawa, Adv. At. Mol. Phys. **6**, 105 (1970).
[3] K. Takayanagi, in *Electronic and Atomic Collisions*, edited by I. Shimamura and K. Takayanagi (Plenum, New York, 1984).
[4] J. Randell, J.-P. Ziesel, S. L. Lunt, G. Mrotzek, and D. Field, J. Phys. B **26**, 3423 (1993).
[5] J. Randell, R. J. Gulley, S. L. Lunt, J.-P. Ziesel, and D. Field, J. Phys. B **29**, 2049 (1996).
[6] R. J. Gulley, T. A. Field, W. A. Steer, N. J. Mason, S. L. Lunt, J.-P. Ziesel, and D. Field, J. Phys. B **31**, 5197 (1998).
[7] S. L. Lunt, D. Field, S. V. Hoffman, R. J. Gulley, and J.-P. Ziesel, J. Phys. B **32**, 2707 (1999).
[8] D. Field, N. C. Jones, J. M. Gingell, N. J. Mason, S. L. Lunt, and J.-P. Ziesel, J. Phys. B **33**, 1039 (2000).
[9] S. L. Lunt, D. Field, J.-P. Ziesel, N. C. Jones, and R. J. Gulley, Int. J. Mass. Spectrom. **205**, 197 (2001).
[10] D. Field, S. L. Lunt, and J. P. Ziesel, Acc. Chem. Res. **34**, 291 (2001).
[11] R. Curik, J.-P. Ziesel, N. C. Jones, T. A. Field, and D. Field, Phys. Rev. Lett. **97**, 123202 (2006).
[12] N. C. Jones, D. Field, and J.-P. Ziesel, Int. J. Mass Spectrom. (to be published).
[13] Y. Itikawa and N. J. Mason, Phys. Rep. **414**, 1 (2005).
[14] D. Field, D. F. Klemperer, P. W. May, and Y. P. Song, J. Appl. Phys. **70**, 82 (1991).
[15] Y. P. Song, D. Field, and D. F. Klemperer, J. Phys. D **23**, 673 (1990).
[16] D. Field *et al.*, in *Proceedings, Molecules in Space & Laboratory, Paris, 2007*, edited by J. L. Lemaire and F. Combes (unpublished).
[17] R. Balog, P. Cicman, L. Feketeova, K. Hoydalsvik, N. C. Jones, T. A. Field, J.-P. Ziesel, and D. Field (unpublished).
[18] A. Faure, J. D. Gorfinkiel, and J. Tennyson, J. Phys. B **37**, 801 (2004).
[19] A. Faure, J. D. Gorfinkiel, and J. Tennyson, Mon. Not. R. Astron. Soc. **347**, 323 (2004).
[20] F. A. Gianturco, J. Phys. B **24**, 4627 (1991).
[21] J. Yuan and Z. Zhang, Phys. Rev. A **45**, 4565 (1992).
[22] T. N. Rescigno, B. H. Lengsfield, C. W. McCurdy, and S. D. Parker, Phys. Rev. A **45**, 7800 (1992).
[23] M. H. F. Bettega, M. A. P. Lima, and L. G. Ferreira, Phys. Rev. A **70**, 062711 (2004).
[24] M. H. F. Bettega, M. A. P. Lima, and L. G. Ferreira, Phys. Rev. A **72**, 014702 (2005).
[25] H. Munjal and K. L. Baluja, Phys. Rev. A **74**, 032712 (2006).
[26] M. Gupta and K. L. Baluja, Eur. Phys. J. D **41**, 475 (2007).
[27] F. A. Gianturco and T. Stoecklin, Chem. Phys. **332**, 145 (2007).
[28] D. Field, D. W. Knight, S. L. Lunt, G. Mrotzek, J.-B. Ozenne, and J.-P. Ziesel, Meas. Sci. Technol. **2**, 757 (1991).
[29] D. Field, N. C. Jones, S. L. Lunt, and J.-P. Ziesel, Phys. Rev. A

64, 022708 (2001).
[30] S. V. Hoffmann, S. L. Lunt, N. C. Jones, D. Field, and J.-P. Ziesel, Rev. Sci. Instrum. **73**, 4157 (2002).
[31] K. Radler and J. Berkowitz, J. Chem. Phys. **70**, 221 (1979).
[32] W. G. Sun, M. A. Morrison, W. A. Isaacs, W. K. Trail, D. T. Alle, R. J. Gulley, M. J. Brennan, and S. J. Buckman, Phys. Rev. A **52** 1229 (1995).
[33] J. Randell, S. L. Lunt, G. Mrotzek, J.-P. Ziesel, and D. Field, J. Phys. B **27**, 2369 (1994).
[34] K. Rohr, J. Phys. B **10**, 1175 (1977).
[35] R. E. Kennerly, Phys. Rev. A **21**, 1876 (1980).
[36] J. Randell, D. Field, S. L. Lunt, G. Mrotzek, and J. P. Ziesel, J. Phys. B **25**, 2899 (1992).
[37] K. Floeder, D. Fromme, W. Raith, A. Schwab, and G. Sinapius, J. Phys. B **18**, 3347 (1985).
[38] K. Rohr, J. Phys. B **11**, 4109 (1978).
[39] E. Gerjuoy and S. Stein, Phys. Rev. **97**, 1671 (1955).
[40] T. Nishimura and Y. Itikawa, J. Phys. B **29**, 4213 (1996).
[41] *Landolt-Bornstein New Series* (Springer-Verlag, Berlin, 2003).
[42] O. Sueoka, S. Mori, and Y. Katayama, J. Phys. B **20**, 3237 (1987).
[43] C. Szmytkowski, K. Maciag, G. Karwasz, and D. Filipovic, J. Phys. B **22**, 525 (1989).
[44] D. Y. Alle, R. J. Gulley, S. J. Buckman, and M. J. Brunger, J. Phys. B **25**, 1533 (1992).
[45] C. Szmytkowski, A. Domaracka, P. Mozejko, E. Ptasinska-Denga, L. Klosowski, M. Piotrowicz, and G. Kasperski, Phys. Rev. A **70**, 032707 (2004).
[46] S. L. Lunt, J. Randell, J.-P. Ziesel, G. Mrotzek, and D. Field, J. Phys. B **31**, 4225 (1998).
[47] R. J. Gulley, M. J. Brunger, and S. J. Buckman, J. Phys. B **26**, 2913 (1993).
[48] C. Szmytkowski and K. Maciag, Chem. Phys. Lett. **129**, 321 (1986).
[49] C. Szmytkowski, P. Mozejko, and A. Krsysztofowicz, Radiat. Phys. Chem. **68**, 307 (2003).
[50] A. Jain and D. G. Thompson, J. Phys. B **17**, 443 (1984).
[51] P. Rawat, I. Iga, M.-T. Lee, L. M. Brescansin, M. G. P. Homem, and L. E. Machado, Phys. Rev. A **68**, 052711 (2003).
[52] C. Szmytkowski and M. Zubek, Chem. Phys. Lett. **57**, 105 (1978).
[53] C. Szmytkowski, G. Karwasz, and K. Maciag, Chem. Phys. Lett. **107**, 481 (1984).
[54] W. Sohn, K-H. Kochem, K. M. Scheuerlein, K. Jung, and H. Ehrhardt, J. Phys. B **20**, 3217 (1987).
[55] O. Sueoka, A. Hamada, M. Kimura, H. Tanaka, and M. Kitajima, J. Chem. Phys. **111**, 245 (1999).
[56] G. Karwasz, T. Wroblewski, R. S. Brusa, and E. Illenberger, Jpn. J. Appl. Phys., Part 1 **45**, 8192 (2006).
[57] D. Field, J.-P. Ziesel, S. L. Lunt, R. Parthasarathy, L. Suess, S. B. Hill, B. Dunning, R. R. Lucchese, and F. A. Gianturco, J. Phys. B **34**, 4371 (2001).
[58] D. Field, N. C. Jones, and J.-P. Ziesel, Phys. Rev. A **69**, 052716 (2004).
[59] N. C. Jones, D. Field, J.-P. Ziesel, and T. A. Field, Phys. Rev. Lett. **89**, 093201 (2002).
[60] T. Suzuki, H. Katayanagi, S. Nanbu, and M. Aoyagi, J. Chem. Phys. **109**, 5778 (1998).
[61] G. L. Gutsev, R. J. Bartlett, and R. N. Compton, J. Chem. Phys. **108**, 6756 (1998).
[62] E. Surber, S. P. Aanathavel, and A. Sanov, J. Chem. Phys. **116**, 1920 (2002).
[63] T. F. O'Malley, Phys. Rev. **130**, 1020 (1963).
[64] A. Herzenberg and B. C. Saha, J. Phys. B **16**, 591 (1983).
[65] I. I. Fabrikant and R. S. Wilde, J. Phys. B **32**, 235 (1999).
[66] W. Vanroose, C. W. McCurdy, and T. N. Rescigno, Phys. Rev. A **68**, 052713 (2003).
[67] M. A. Morrison, Phys. Rev. A **25**, 1445 (1982).
[68] S. Barsotti, T. Sommerfeld, M.-W. Ruf, and H. Hotop, Int. J. Mass. Spectrom. **233**, 181 (2004).